Progress of Theoretical Physics, Vol. 39, No. 6, June 1968

Rapid Contraction of a Protostar to the Stage of Quasi-Hydrostatic Equilibrium. I

— The Case of One Solar Mass without Radiation Flow —

Takenori NAKANO, Noboru OHYAMA*
and
Chushiro HAYASHI**

Research Institute for Fundamental Physics, Kyoto University, Kyoto
**Department of Physics, Hiroshima University, Hiroshima*
***Department of Physics, Kyoto University, Kyoto*

(Received February 17, 1968)

The evolution of an opaque protostar of one solar mass is investigated up to the onset stage of quasi-hydrostatic equilibrium by solving numerically the hydrodynamic equations of motion. The protostar is assumed to retain spherical symmetry. The dissipation of the energy of mass motion by shock waves is taken into account, but the radiation flow in the protostar is neglected because of the rapidity of the dynamics. It is found that the stellar structure at the onset stage of quasi-hydrostatic equilibrium is insensitive to the initial distributions of density and temperature in the protostar. At this onset stage the star has an isothermal and dense core and a tenuous envelope with a radius of about $200R_\odot$. By the shock wave an outermost envelope having a mass as small as $10^{-4}M_\odot$ is ejected from the star.

§ 1. Introduction

Recently a number of infrared objects have been discovered in the disk of our galaxy,[1),2)] and some of them are known to have bolometric luminosities as high as $10^3L_\odot$.[3),4)] An attractive interpretation of the observations is that the central and main bodies of the infrared objects are protostars which have flared up at the last stage of their dynamical contraction. For example, R Mon has been interpreted by Low and Smith[3)] as being composed of a central flared-up star and a surrounding dust cloud which is converting the visible radiation from the central star into the infrared radiation. The study of the evolution of such a protostar will also be important in connection with the origin of the solar system.

In a previous work, Hayashi and Nakano (to be referred to as HN) have examined theoretically the dynamical and the thermal behavior of a protostar of one solar mass, which has once been formed from the interstellar medium.[5)] Under the assumption that the protostar retains both spherical symmetry and mass, they have found the general features of its evolution in transparent and

opaque stages up to the onset of quasi-hydrostatic equilibrium, i.e. up to the beginning of the pre-main-sequence slow contraction. The main results of this study have also been summarized by Hayashi.[6]

According to the above study, the initial stage of the opaque protostar, from which an adiabatic contraction begins, is determined mainly by the cooling effect of grains, almost irrespective of its previous history. The mean density and temperature of this initial state are about 4×10^{-14}g/cm^3 and 15°K, respectively, for the star of one solar mass. The corresponding pressure is too low by a factor of more than 20 to maintain gravitational equilibrium.

Thus, the opaque protostar undergoes rapid contraction until the total thermal energy becomes comparable to the gravitational energy so that quasi-hydrostatic equilibrium is finally established. At this last stage the contraction is stopped by the bounce of a central core and by the shock waves, which are produced by the bounce itself and propagate towards the surface. These shock waves are expected to give rise to a sudden flare-up of the star to a luminosity above $3\times10^2L_\odot$, as observed in the infrared stars.

As mentioned above, many features of the evolution have been found in HN, but the hydrodynamic process after the bounce of a core has not been computed numerically. Thus, there remain many questions to be clarified quantitatively such as the strength of the shock waves, the amounts of energy dissipation and mass ejection by the shock waves, the stellar structure and the luminosity at the time of the flare-up, etc.

The purpose of the present paper is to answer the above questions by solving the hydrodynamic equations directly with an electronic computer for the opaque protostar of one solar mass. The effect of shock waves, such as the energy dissipation, has been described in terms of von Neumann and Richtmyer's artificial viscosity.[7] However, the energy flow by radiation has been neglected completely. Because of the rapid contraction, this energy flow is negligible in the bulk of the star, except for the immediate neighborhood of the surface.*)

In § 2, the basic formulation of the hydrodynamic problem will be described. The detailed reformulation of differential equations into difference equations will be given in Appendix I. Also, the equation of state and the other thermodynamical relations, which appear in the hydrodynamic equations, will be described in Appendix II, together with the formulae for the dissociation of hydrogen molecules and for the ionization of hydrogen and helium atoms.

In § 3, the results of the computation will be described. The computations have been performed for different distributions of the initial density and temperature (or entropy) in the protostar, because only their mean values have been obtained in HN. Further, for the chemical composition, we have considered the two cases, the case of pure hydrogen and the case of a mixture of hydrogen

*) The results of the computation in which the energy flow by radiation is included will be described in a forthcoming paper.

(70 per cent by mass) and helium (30 per cent by mass).

The results of the computations show that the stellar structure at the onset stage of quasi-hydrostatic equilibrium is almost independent of the initial distributions of the density and temperature; it is of centrally condensed type having a nearly isothermal core. The mass ejected at the time of the flare-up is as small as $10^{-4}M_\odot$ (the case of pure hydrogen) or $10^{-5}M_\odot$ (the case of hydrogen and helium).

Finally, in § 4, discussion will be made on the result that the final equilibrium structure is insensitive to the initial configuration and also on the validity of the assumption of the negligible radiation flow.

§ 2. Hydrodynamic equations

The existence of double stars and that of planets in the solar system indicates that the angular momentum played an important role in the formation process of these objects. However, if we restrict ourselves to the consideration of the central main body of a single star system, there may be many cases in which the effect of the angular momentum on the evolution was not essential. This is one of the reasons why in this paper the protostar is assumed to be spherically symmetric, and another reason is the simplicity of the computations.

Furthermore, in this paper the energy flow by radiation in the protostar is neglected since, after the optical thickness of the star has become much greater than unity, the time-scale of energy loss by radiation in the bulk of the star is much greater than the time-scale of contraction.

Now, in the Lagrangian scheme, where t(time) and m(mass contained in a sphere of radius r) are taken as independent variables, the equation of motion is given by

$$\frac{\partial u}{\partial t}=-4\pi r^2\frac{\partial}{\partial m}(P+Q)-\frac{Gm}{r^2}, \tag{1}$$

$$\frac{\partial r}{\partial t}=u, \tag{2}$$

where u is the velocity, P is the pressure and Q is von Neumann and Richtmyer's artificial viscosity which describes the dissipation of kinetic energy into thermal energy by shock waves. The expression for Q is given by

$$Q=\begin{cases}\dfrac{l^2}{v}\left(\dfrac{\partial u}{\partial r}\right)^2, & \text{if } \dfrac{\partial u}{\partial r}<0 \text{ and } \dfrac{\partial v}{\partial t}<0,\\ 0, & \text{otherwise,}\end{cases} \tag{3}$$

where v is the specific volume and l is a constant having the dimension of length.[7] Further, for the specific volume v or the density ρ, we have the equation of continuity of mass

$$v \equiv \frac{1}{\rho} = \frac{\partial}{\partial m}\left(\frac{4\pi}{3} r^3\right). \tag{4}$$

Since the pressure P is a function of the density ρ and the temperature T, we need one more equation which describes the time variation of the temperature. This equation is given by the energy conservation law, which is expressed as

$$\frac{\partial T}{\partial t} = -\frac{P + Q + (\partial \varepsilon / \partial v)_T}{(\partial \varepsilon / \partial T)_v} \frac{\partial v}{\partial t}, \tag{5}$$

where ε is the internal energy per unit mass, which is considered as a function of v and T, and the energy flow by radiation has been neglected.

When both P and ε are given as functions of v and T, the initial-value problem is completely described by a set of Eqs. (1) to (5). The reformulation of these equations into difference equations, which have been used in the present computations, is described in Appendix I. This reformulation is essentially the same as that made by Colgate and White[8] and Arnett[9] in the investigation of the supernova explosion.

Furthermore, the equations of state which have been used in the present computations are summarized in Appendix II.

§ 3. Numerical results

As an initial stage for the computation we choose a stage when the protostar has become sufficiently opaque but the pressure is still so low that the contraction is an adiabatic free-fall. As shown in HN, in such a stage the mean specific entropy of the protostar depends only on the stellar mass, irrespective of the previous history of its evolution, and for the protostar of one solar mass we have

$$\langle v \rangle \langle T \rangle^{5/2} \approx 10^{16}, \tag{6}$$

where the brackets denote the mean values and v and T are in units of cm^3/g and °K, respectively. It has been found in HN that the protostar of one solar mass becomes opaque at a stage when $R \approx 3 \times 10^4 R_\odot$. Then, it is sufficient to choose as the initial radius $R_0 = 5 \times 10^3 R_\odot$, for which we have $\langle v_0 \rangle \approx 10^{11} \mathrm{cm}^3/\mathrm{g}$ and $\langle T_0 \rangle \approx 10^{2}$°K from Eq. (6).

The distributions of the density and the temperature in this initial stage depend generally on the previous history of evolution. Therefore several possible cases have to be considered. As to the density distribution we consider the two cases: one is the distribution represented by the Emden solution of the polytropic index $N = 1.5$ (relatively uniform distribution) and the other is that of the polytropic index $N = 4$ (centrally condensed distribution). As to the temperature distribution, we consider an isothermal case, an isentropic case and also a case intermediate between the two. Further, as to the chemical com-

position of the protostar, we consider the case of pure hydrogen and also the case of a mixture of hydrogen (70 per cent by mass) and helium (30 per cent by mass).*)

Among the possible cases mentioned above, the evolution has been computed in detail for the four cases: (1) initially $N=1.5$ and isentropic (pure hydrogen), (2) initially $N=1.5$ and isothermal (pure hydrogen), (3) initially $N=4$ and intermediate between isothermal and isentropic (pure hydrogen), and (4) the same initial conditions as case 3 (the mixture of hydrogen and helium).

In all of the above cases, as the initial velocities of the shells we take $u_0=-(2Gm/r_0)^{1/2}$, i.e. the velocities obtained through the free fall from infinity to the present radius r_0. The computations have been made on electronic computers IBM 7090 and HITAC 5020E. The results for each of the four cases will be described in what follows.

Case 1 (*initially*, $N=1.5$ *and isentropic*; *pure hydrogen*)

The initial density distribution is given by the Emden solution of index 1.5. As the initial central temperature T_c we take 200°K. Then, the initial isentropic distribution is expressed as

$$T/T_c=(\rho/\rho_c)^{2/5}, \tag{7}$$

Table I. The shell numbers j, the fractional masses m/M and the initial fractional radii r_0/R_0 of the typical shells.

j	$N=1.5$		$N=4$	
	m/M	r_0/R_0	m/M	r_0/R_0
3	0.005875	0.1	0.06312	0.050
6	0.04426	0.2	0.3043	0.100
9	0.1353	0.3	0.5636	0.150
12	0.2798	0.4	0.7448	0.200
15	0.4600	0.5	0.8544	0.250
18	0.6465	0.6	0.9274	0.311
21	0.8090	0.7	0.9773	0.410
24	0.9252	0.8	0.9962	0.550
27	0.9860	0.9	0.9998	0.730
30	1.0000	1.0	1.0000	1.000

because hydrogen are all in a molecular state at such low temperatures. This distribution gives a reasonable surface temperature of about 20°K.

In computations the protostar has been divided into 30 shells. The fractional masses m/M and the initial radii of several shells are shown in Table I. The

*) The presence of heavier elements having a concentration by mass as small as 0.03 can be neglected in the present treatment where the radiation flow has been neglected, since their contribution to the equations of state is very small.

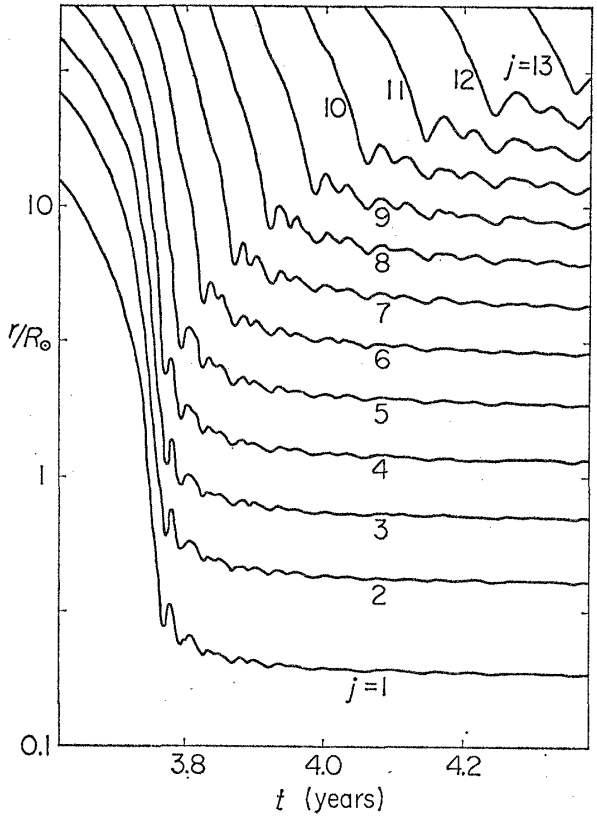

Fig. 1. The time variation of the radii of the inner shells for the initial configuration of case 1 (N=1.5 and isentropic; pure hydrogen). The shell numbers are denoted by j.

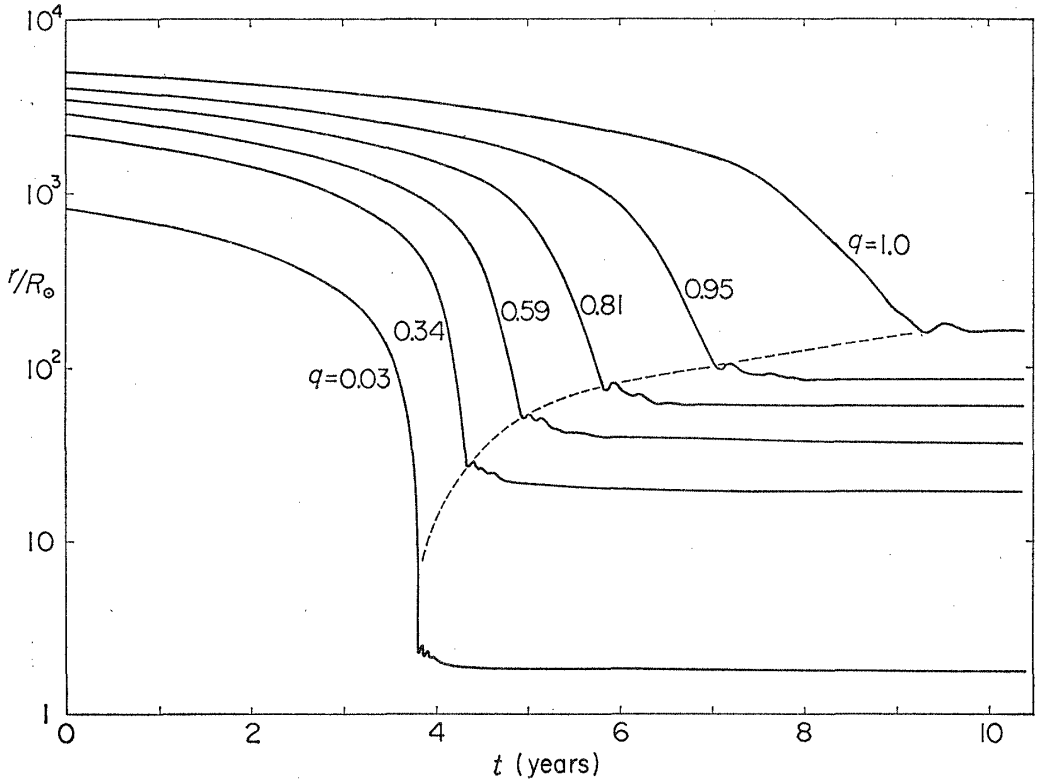

Fig. 2. The time variation of the radii of typical shells from the initial stage to the onset stage of quasi-hydrostatic equilibrium for case 1. The fractional masses m/M of the shells are denoted by q. The dashed curve represents the path of propagation of the shock front.

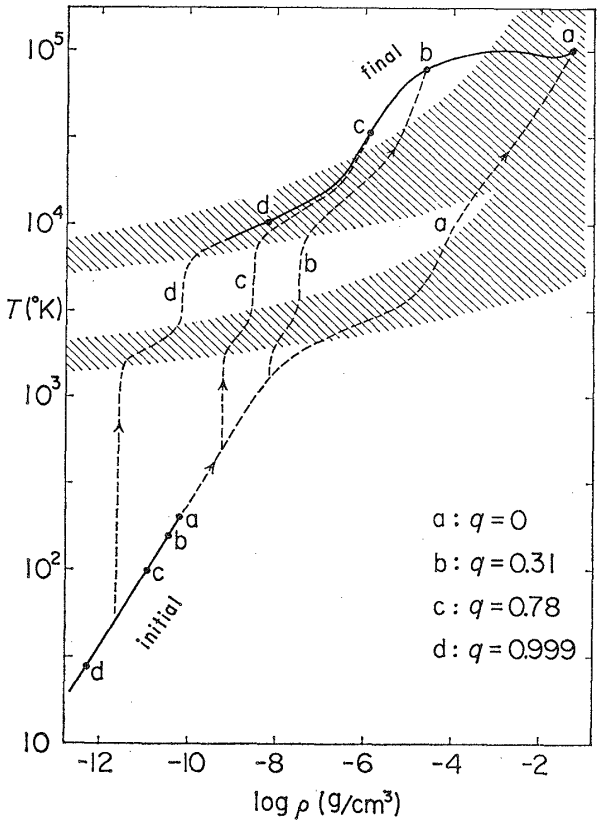

Fig. 3. The evolutionary paths (the dashed curves) of four typical shells (denoted by a, b, c and d) in the density-temperature diagram for case 1. The initial and final structures are shown by the solid curves and the closed circles. The hatched regions are the ionization zone of hydrogen atoms (upper) and the dissociation zone of hydrogen molecules (lower).

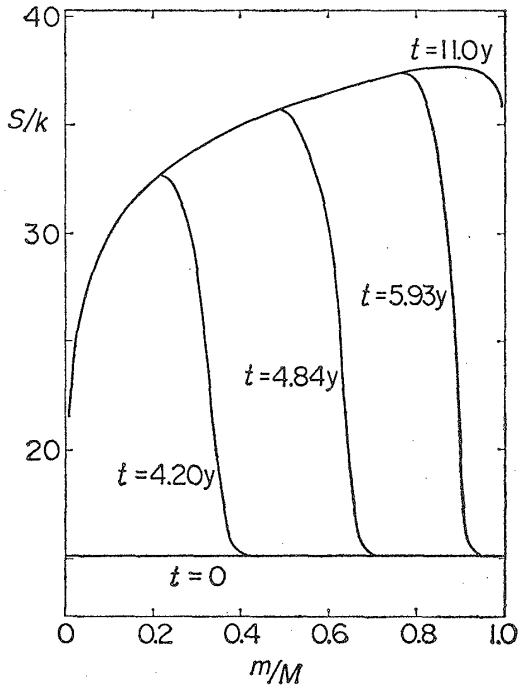

Fig. 4. The distributions of the entropy S (per one atomic mass) in the protostar at four different stages of case 1. The abscissa is the mass fraction, the time t is in years and k is the Boltzmann constant.

computations have also been made with the division into 60 shells. By comparing the results of 30 shells with those of 60 shells, we have found that the corresponding shells show very similar evolution and finally settle down to the same equilibrium state (concerning the radius, the temperature, etc.), except for a slight difference in a few innermost shells. Thus, the division of the protostar into 30 shells is satisfactory.

The details of the contraction and bounce of the inner shells in the relatively early stages are shown in Fig. 1. The over-all time variation of the radii of typical shells from the initial stage to the onset of quasi-hydrostatic equilibrium is shown in Fig. 2, where the path of the shock front is denoted by the dashed curve. In Fig. 3, the evolutionary paths of four typical shells in the density-temperature diagram are shown by the dashed curves, together with the initial and final states denoted by the closed circles and the solid curves.

Figure 4 shows the distribution of the entropy S per one atomic mass at several stages. The whereabouts of the shock front is represented by the regions where the entropy changes greatly. In reality the thermodynamical quantities such as temperature, density and entropy are to be discontinuous across the shock front. However, in the difference method using von Neumann and Richtmyer's artificial viscosity, the shock front contains a few shells and has a small but finite thickness as shown in Fig. 4.[7)]

After the arrival of the shock wave to the surface region, the star is in quasi-hydrostatic equilibrium. As is shown in Fig. 2, the surface ($q=1.0$) settles down finally to a radius $R\approx 170\,R_\odot$, and there has been no indication of mass ejection despite the heating by the shock wave. Then, we can conclude that the ejected mass is much smaller than $10^{-3}M_\odot$ which is the mass of the outermost shell adopted in the present computation. In order to find the amount of the ejected mass, it is necessary to divide the outermost region into much more shells (see the results of cases 3 and 4 below).

The distributions of temperature, density and entropy at the onset stage of quasi-hydrostatic equilibrium are shown by the solid curves in Figs. 5, 6 and 7, respectively, where the results for the other cases 2, 3 and 4 are added for comparison. The central temperature is about $10^{5\circ}$K and hydrogen is completely ionized in the bulk of the star. The reason for the formation of a nearly isothermal core, as seen in Fig. 3, will be explained as follows.

In the early phase of free-fall contraction the kinetic energy per unit mass near the center is given by

$$\frac{Gm}{r}\approx G\rho r^2, \tag{8}$$

which tends to vanish at the center. Then, in the shells nearer to the center, the gain of entropy by the dissipation of this energy by the shock wave is smaller. This low entropy of the central region gives rise to the nearly isothermal and highly dense core.

Now, we define the local polytropic index n by*)

$$\frac{d\log P}{d\log \rho}=1+\frac{1}{n}. \tag{9}$$

The distribution of $d\log P/d\log\rho$ in the star at the onset stage of quasi-hydrostatic equilibrium is shown by the solid curve in Fig. 8. The polytropic index n is large in the inner regions and small in the outer regions. Near the center we have even a negative value of n which corresponds to the reversed temperature gradient. If we define the mean polytropic index $<n>$ of the star by taking the mass average of $d\log P/d\log\rho$ in Eq. (9) we have

*) We distinguish the polytropic index n from the index N which characterizes the initial density distribution but has no relation to the pressure distribution.

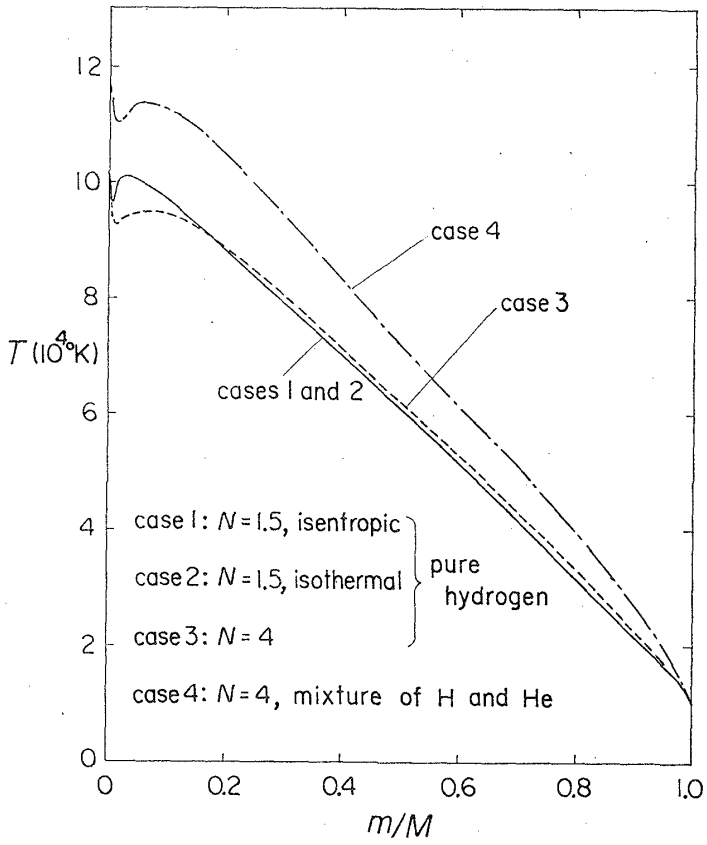

Fig. 5. The temperature distributions in the star at the onset stage of quasi-hydrostatic equilibrium. The solid curve represents the results for cases 1 and 2, the dashed curve is for case 3 and the dot-dashed curve is for case 4.

$$<n>=4.1\,. \tag{10}$$

We shall compare the equilibrium structure, which has been described in the above, with that of a polytrope of a constant index n. In the case of the polytrope, we have from the energy conservation during the contraction[5),6)]

$$\frac{1}{2}\,\frac{3}{5-n}\,\frac{GMH}{R}=\frac{\chi_1}{2}+\chi_2, \tag{11}$$

where H is the mass of the hydrogen atom and χ_1 and χ_2 are the dissociation energy of a hydrogen molecule and the ionization energy of a hydrogen atom, respectively. If we adopt the computed value of $R(=170R_\odot)$ in Eq. (11), we have $n=3.9$. It is to be noticed that this value is in good agreement with the mean value of the local polytropic index given by Eq. (10).

Case 2 (*initially*, $N=1.5$ *and isothermal*; *pure hydrogen*)

As the initial temperature we take $T_0=100°$K throughout the protostar. The other initial conditions and the division of the protostar are the same as

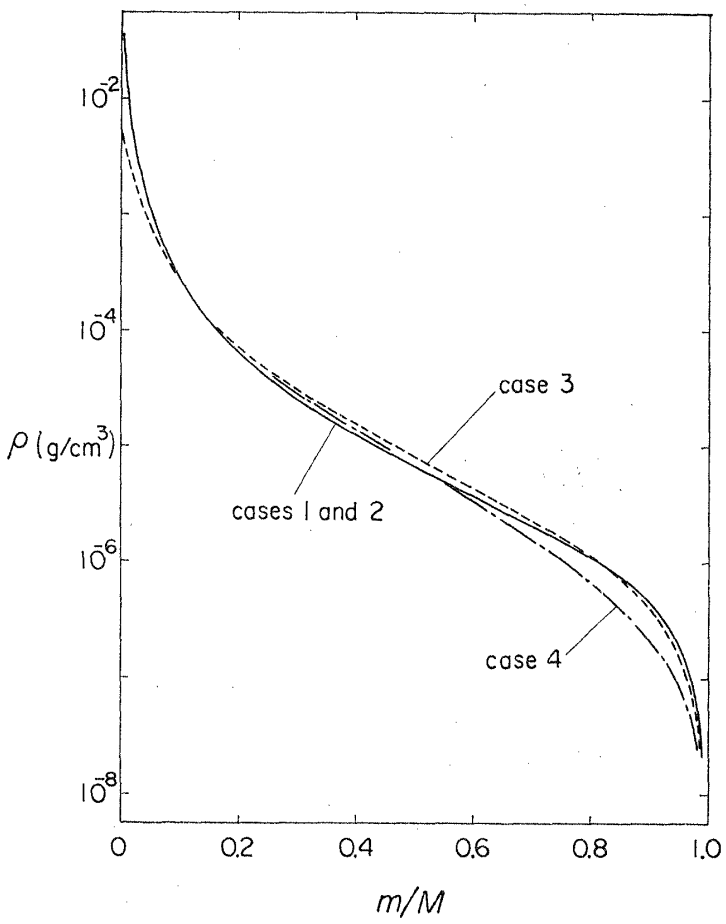

Fig. 6. The density distributions in the star at the onset stage of quasi-hydrostatic equilibrium. The notations are the same as in Fig. 5. The dashed curve and the dot-dashed curve are indistinguishable for $m/M<0.25$.

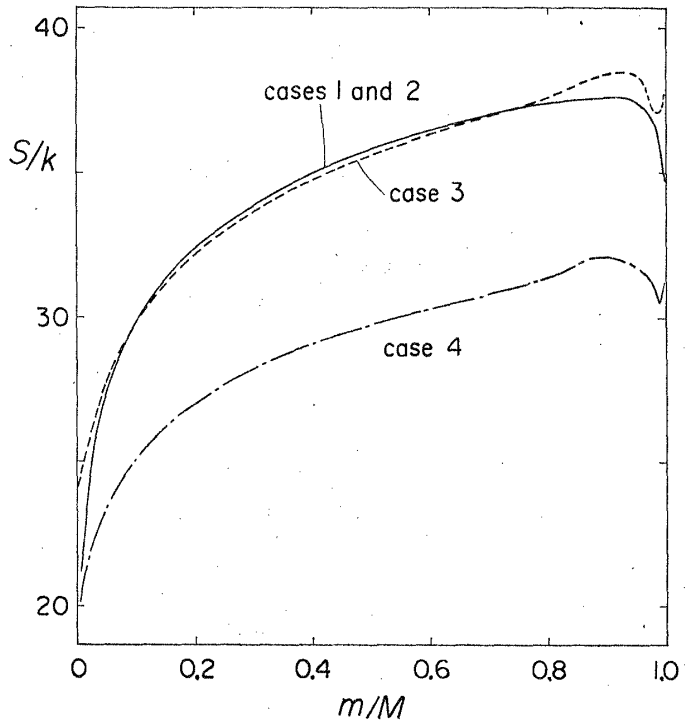

Fig. 7. The distributions of the entropy S (per one atomic mass) in the star at the onset stage of quasi-hydrostatic equilibrium. The notations are the same as in Fig. 5.

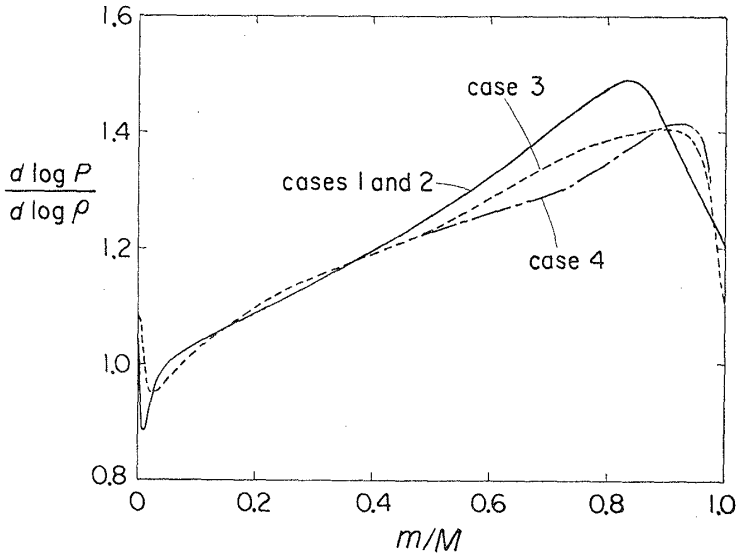

Fig. 8. The distributions of $d\log P/d\log\rho$ in the star at the onset stage of quasi-hydrostatic equilibrium. The notations are the same as in Fig. 5. The dashed curve and the dot-dashed curve are indistinguishable for $m/M<0.5$.

case 1.

Because the pressure effect is negligibly small as compared to the gravitational force in the early stages, the protostar contracts essentially in the same way as in case 1, and finally establishes a quasi-hydrostatic equilibrium with a radius of about $170R_\odot$. The structure of the star in this equilibrium state is shown in Figs. 5, 6, 7 and 8 by the solid curves, which are indistinguishable from those of case 1 in all of these diagrams. This equality of the final structure in cases 1 and 2 can be explained as follows. The final thermal energy of each shell, which has been acquired through the dissipation of the kinetic energy, is insensitive to the initial temperature because the initial thermal energy is much smaller than the kinetic energy.

Case 3 (*initially*, $N=4$; *pure hydrogen*)

The initial density distribution is represented by the Emden solution of index 4. The results of cases 1 and 2 show that the initial temperature distribution is not important in determining the contraction process and the final structure of the protostar. Then, we assume, for simplicity, the initial temperature distribution, which is intermediate between the isothermal and the isentropic cases,

$$T/T_c=(\rho/\rho_c)^{0.2} \tag{12}$$

with $T_c=100°\mathrm{K}$. This distribution gives a reasonable temperature of about 20°K for a shell of a unit optical depth (the opacity due to grains[5] having been adopted). We divide the protostar into 30 shells. The fractional masses m/M and the initial radii of some typical shells are shown in Table I.

The time variation of the radii of some typical shells is shown in Fig. 9. After the passage of the shock wave through the star, the outermost region containing a mass of about $10^{-4}M_{\odot}$ escapes from the star with a velocity greater than the escape velocity. The remaining part of the star settles down to a state of quasi-hydrostatic equilibrium with a radius of about $200R_{\odot}$.

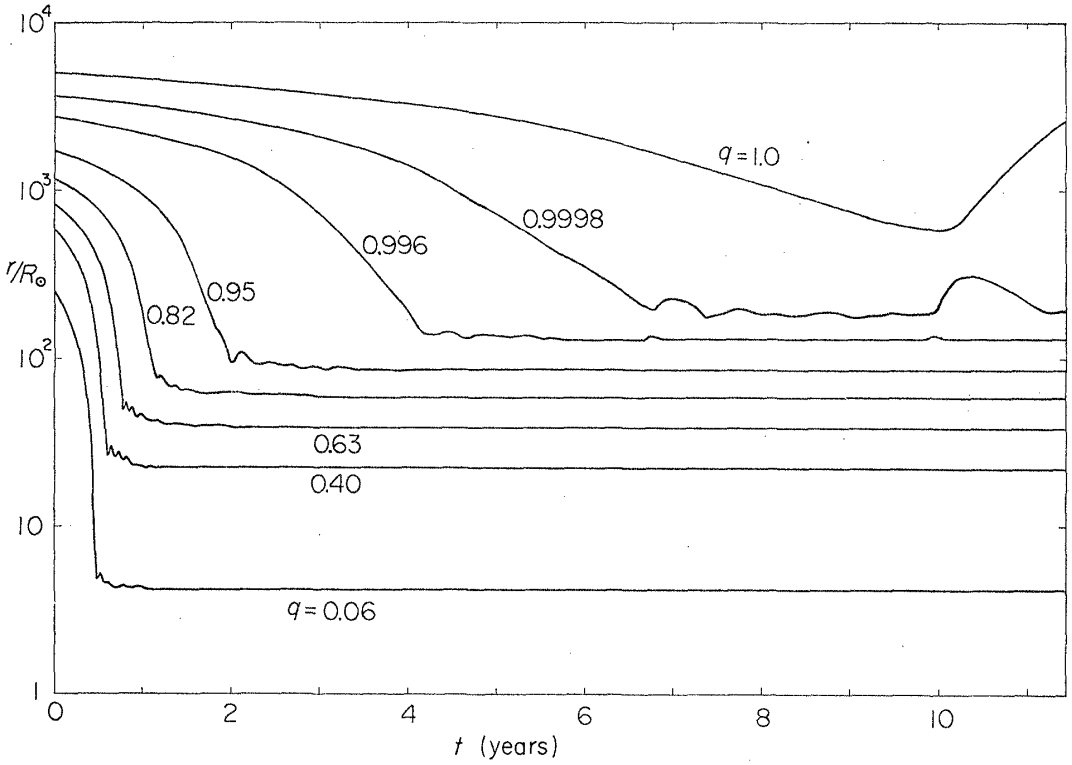

Fig. 9. The time variation of typical shells from the initial stage to the onset stage of quasi-hydrostatic equilibrium for case 3. The fractional masses of the shells are denoted by q.

The features of this equilibrium structure, which are shown by the dashed curves in Figs. 5, 6, 7 and 8, are very similar to those in cases 1 and 2. For the mean polytropic index, we have $<n>=4.3$. In the central region, there is some difference from cases 1 and 2. This is due to the different way of division of the protostar in this region. Such a difference has already been found in case 1 between the cases of 30 shells and 60 shells division. Also, in the surface region, the distributions of the entropy and $d\log P/d\log\rho$ are slightly different from those of cases 1 and 2. These differences seem to be due mainly to the different way of division of the protostar in the surface region.

From the results of cases 1, 2 and 3 described above, we can conclude that the structure of the protostar when the quasi-hydrostatic equilibrium is established is insensitive to the details of its initial configuration as long as the condition of Eq. (6) is satisfied. This corresponds to the fact that the velocity of each shell just before the time of its bounce is almost independent of the initial

configuration.

Case 4 (*initially*, $N=4$; *mixture of hydrogen and helium*)

We consider a protostar which is composed of hydrogens (70 per cent by mass) and heliums (30 per cent). The other initial conditions are completely the same as case 3.

We have found that the ejected mass is about $10^{-5}M_{\odot}$, which is much smaller than in case 3. The reason for this is that more energy is consumed in the ionization of helium than in the case of pure hydrogen. The radius of the star at the onset stage of quasi-hydrostatic equilibrium is about $230R_{\odot}$.

The structure of the star when the quasi-hydrostatic equilibrium is established is shown by the dot-dashed curves in Figs. 5, 6, 7 and 8. In this state the single ionization of helium atoms is complete in the inner region where $m/M\leq 0.85$, while the double ionization is incomplete throughout the star. For instance, at the shell of $m/M=0.5$, only about 60 per cent of helium is doubly ionized. The temperature (as seen in Fig. 5) is higher than those of the above three cases of pure hydrogen. This is due mainly to the difference in the mean molecular weight. The distributions of density (Fig. 6) and $d\log P/d\log\rho$ (Fig. 7) show deviations from those of case 3 in the region where $m/M>0.5$. This is the result of the partial ionization of helium. From the mean value of $d\log P/d\log\rho$ we have $<n>=4.6$ for the mean polytropic index.

§ 4. Discussion

As was described in § 3, the structure of the protostar which has finally established the quasi-hydrostatic equilibrium is almost independent of its initial distributions of the density and the temperature. This independence will be seen more clearly in Fig. 10, which shows that the difference in the radius distribution between cases 1 and 3 is greatly reduced in the final stage.

The above equality of the final structure will be due mainly to the fact that the contraction factor of each shell is very large (i.e., $r/r_0\ll 1$, where r_0 and r are the initial and final radius of the shell) and, consequently, the kinetic energy or the gravitational energy Gm/r of the shell, which has been dissipated into the thermal energy, is much greater than any of the thermal energy, the kinetic energy and the gravitational energy Gm/r_0 in the initial stage. If the above reasoning is correct, we can say more generally the final equilibrium structure is almost independent of the initial value of the mean specific entropy, i.e. the value of Eq. (6), as well as the initial distributions of the density and the temperature, as long as the initial pressure is sufficiently small as compared to the pressure which is required to sustain the protostar against its gravity, i.e. as long as the initial state lies sufficiently below the equilibrium line in the temperature-density diagram as shown in Fig. 4 of HN.

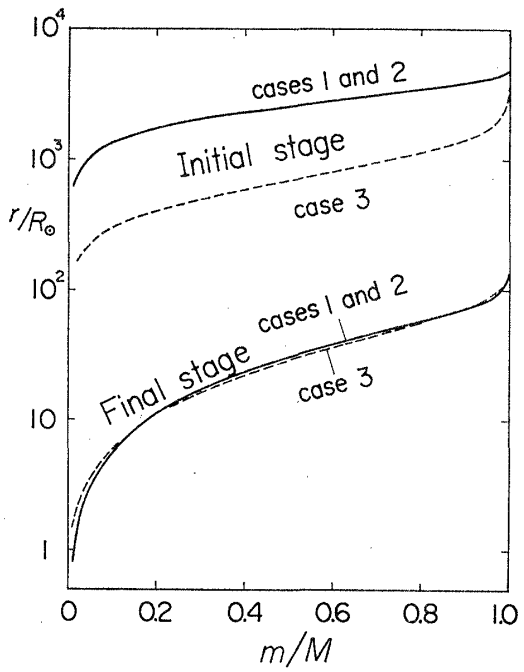

Fig. 10. The relation between the radius r and the mass fraction m/M in the initial stage and the onset stage of quasi-hydrostatic equilibrium for cases 1, 2 and 3.

The effect of the radiation flow in the protostar has been completely neglected in this paper. Apparently, this is a good approximation for the bulk of the protostar, unless the opacity is quite low. At temperatures between 1500°K and 2000°K, the grains have been evaporated and the contribution of molecules to the opacity is still so small that the opacity is quite low. Even if the temperature of some shells lies in this region of low opacity in some stages of evolution, the cooling of the shells due to their good transparency is negligibly small, because the low opacity of a gas means also its low emissivity of radiation and the time of duration of the low opacity is very short in the free-fall contraction.

However, for the surface region which is always optically thin, the effect of radiation flow on the cooling or heating of this region cannot be neglected. The change in the luminosity with the contraction is determined mainly by the above effect. The computation which includes the radiation flow is now in progress and the preliminary result shows that the protostar flares up to the luminosity as high as $2\times10^3 L_\odot$ when the shock front approaches the surface.

Finally, it is to be noticed that the equations of state described in Appendix II are, strictly speaking, applicable to temperatures sufficiently higher than 85°K which corresponds to the energy spacing of the rotational levels of the hydrogen molecule. We are allowed, however, to use these equations for lower temperatures without errors, because in the stages of such low temperatures the protostar undergoes free-fall contraction.

Acknowledgements

The authors wish to express their thanks to the UNICON branch of Japan Society for the Promotion of Science for the use of an IBM 7090 and to the Computer Centre of the University of Tokyo for the use of a HITAC 5020E. One of the authors (N.O.) wishes to express many thanks to Professor J. P. Cox of the Joint Institute for Laboratory Astrophysics of the University of Colorado for his valuable discussions and encouragement. He is also grateful to the

National Science Foundation, U.S.A., for financial support given to him while he was staying at the Joint Institute for Laboratory Astrophysics from September, 1965 to August, 1966.

Appendix I

Difference equations

We divide the protostar into cocentric spherical shells whose boundaries are numbered 0, 1, 2, $\cdots$, J from the center outward. The physical quantities at the zone boundaries are subscripted j and those at the zone center are subscripted $j+1/2$. The quantities at the n-th stage are superscripted n.

The initial configuration is specified by

$$m_j,\ r_j^0,\ u_j^{-1/2} \text{ and } T_{j-1/2}^0;\ j=1, 2, \cdots, J. \tag{A·1}$$

The mass m_j does not depend on the time in the Lagrangian scheme, and the specific volume is given by

$$v_{j+1/2}^0=\frac{4\pi}{3}\{(r_{j+1}^0)^3-(r_j^0)^3\}/\Delta m_{j+1/2}, \tag{A·2}$$

where

$$\Delta m_{j+1/2}=m_{j+1}-m_j. \tag{A·3}$$

If the quantities at the $(n-1/2)$-th and n-th stages are known, the quantities at the $(n+1/2)$-th and $(n+1)$-th stages are found in the following way. Equations (1), (2) and (4) are rewritten as

$$u_j^{n+1/2}=u_j^{n-1/2}-\frac{Gm_j}{(r_j^n)^2}\Delta t^n-4\pi(r_j^n)^2(P_{j+1/2}^n-P_{j-1/2}^n+Q_{j+1/2}^n-Q_{j-1/2}^n)\frac{\Delta t^n}{\Delta m_j}, \tag{A·4}$$

$$r_j^{n+1}=r_j^n+u_j^{n+1/2}\Delta t^{n+1/2}, \tag{A·5}$$

$$v_{j+1/2}^{n+1}=\frac{4\pi}{3}\frac{(r_{j+1}^{n+1})^3-(r_j^{n+1})^3}{\Delta m_{j+1/2}}, \tag{A·6}$$

where Δt^n and $\Delta t^{n+1/2}$ are the time steps which have the relation

$$\Delta t^n=\frac{1}{2}(\Delta t^{n+1/2}+\Delta t^{n-1/2}), \tag{A·7}$$

and Δm_j is defined in terms of $\Delta m_{j+1/2}$ given in Eq. (A·3) by

$$\Delta m_j=\frac{1}{2}(\Delta m_{j+1/2}+\Delta m_{j-1/2}). \tag{A·8}$$

From Eq. (5) the temperature variation is expressed as

$$T_{j+1/2}^{n+1}=T_{j+1/2}^n-\{P_{j+1/2}^{n+1/2}+Q_{j+1/2}^{n+1/2}+(\partial\varepsilon/\partial v)_{j+1/2}^{n+1/2}\}(v_{j+1/2}^{n+1}-v_{j+1/2}^n)/(\partial\varepsilon/\partial T)_{j+1/2}^{n+1/2}, \tag{A·9}$$

where $P^{n+1/2}_{j+1/2}$, $(\partial\varepsilon/\partial v)^{n+1/2}_{j+1/2}$ and $(\partial\varepsilon/\partial T)^{n+1/2}_{j+1/2}$ are the functions of $v^{n+1/2}_{j+1/2}$ and $T^{n+1/2}_{j+1/2}$ which are given by

$$v^{n+1/2}_{j+1/2}=(1/2)\,(v^{n+1}_{j+1/2}+v^{n}_{j+1/2}), \tag{A·10}$$

$$T^{n+1/2}_{j+1/2}=T^{n}_{j+1/2}+\frac{1}{2}\frac{\Delta t^{n+1/2}}{\Delta t^{n-1/2}}(T^{n}_{j+1/2}-T^{n-1}_{j+1/2}). \tag{A·11}$$

From Eq. (3) the artificial viscosity appearing in Eq. (A·9) is written as

$$Q^{n+1/2}_{j+1/2}=\begin{cases} a^2(u^{n+1/2}_{j+1}-u^{n+1/2}_{j})^2/v^{n+1/2}_{j+1/2}, & \text{if } v^{n+1}_{j+1/2}<v^{n}_{j+1/2} \\ & \text{and } u^{n+1/2}_{j+1}<u^{n+1/2}_{j}, \\ 0, & \text{otherwise,} \end{cases} \tag{A·12}$$

where a is a non-dimensional quantity of the order of unity.[7] In this paper we take $a^2=2$. The artificial viscosity $Q^{n}_{j+1/2}$ in Eq. (A·4) may be given by Eq. (A·12) with n in place of $n+1/2$. In this case we must calculate $u_j{}^n$ by extrapolation. However, because the artificial viscosity has not a firm physical foundation, we define simply

$$Q^{n}_{j+1/2}=Q^{n-1/2}_{j+1/2}. \tag{A·13}$$

The stability of the above difference equations requires that the time step must be smaller than the time in which the sound wave propagates through any of the shells. In the computation of the free-fall contraction phase in which the sound velocity is small, the above condition for the time step is quite insufficient. The changes of the specific volume and the temperature in one time step must be sufficiently small in order to compute the equation of motion and the temperature variation correctly. Then, in this paper we take as the time step $\Delta t^{n+1/2}$ the minimum of the three quantities

$$0.3\frac{r^{n}_{j}-r^{n}_{j-1}}{c^{n}_{j-1/2}},\quad 10^{-2}\frac{v^{n}_{j-1/2}\,\Delta t^{n-1/2}}{|v^{n}_{j-1/2}-v^{n-1}_{j-1/2}|},\quad 10^{-2}\frac{T^{n}_{j-1/2}\,\Delta t^{n-1/2}}{|T^{n}_{j-1/2}-T^{n-1}_{j-1/2}|}$$
$$(j=1,\,2,\,\cdots,\,J), \tag{A·14}$$

where c is the sound velocity.

Appendix II

Equations of state

Concentrations by mass of hydrogen and helium are denoted by X and Y, respectively. The contribution of heavier elements to the equations of state is neglected because of their small concentration, while the contribution of radiation is included in view of applicability to the cases of massive protostars. When the protostar is opaque, the density is so high that the molecules, atoms

and ions of hydrogen and helium are in chemical equilibrium. In the region of temperature and density studied in this paper, the zones of molecular dissociation and atomic ionization are well separated from each other, except for the ionization of hydrogen atoms and the single ionization of helium atoms. The equations of state in each of these zones are described in what follows.

1) *Dissociation of hydrogen molecules*

The dissociation degree x_1 of hydrogen molecules is determined by

$$\frac{x_1^2}{1-x_1}=\frac{H^{5/2}}{2hIX}\left(\frac{kT}{\pi}\right)^{1/2}v(1-e^{-h\nu/kT})e^{-\chi_1/kT}, \tag{A·15}$$

where H is the mass of the hydrogen atom and χ_1, ν and I are the dissociation potential, the vibration frequency and the moment of inertia of the hydrogen molecule, respectively, which have the values

$$\chi_1=4.48\text{eV},\ h\nu/k=6.10\times10^3\text{°K and } h^2/8\pi^2kI=85.4\text{°K}. \tag{A·16}$$

The pressure and the entropy per one atomic mass are given in terms of x_1 by

$$P=\left\{\frac{X}{2}(1+x_1)+\frac{Y}{4}\right\}\frac{kT}{Hv}+\frac{1}{3}aT^4, \tag{A·17}$$

$$S=k\left(X+\frac{Y}{4}\right)\left\{\frac{5}{2}+\ln\frac{2H(2\pi HkT)^{3/2}v}{h^3}\right\}-kX\frac{1-x_1}{2}\left\{\frac{3}{2}+\frac{\chi_1}{kT}-\frac{h\nu/kT}{\exp(h\nu/kT)-1}\right\}$$
$$-kX\ln\frac{x_1X}{2}-\frac{kY}{4}\ln\frac{Y}{16}+\frac{4}{3}aHvT^3. \tag{A·18}$$

The internal energy per unit mass is given by

$$\varepsilon=\frac{X}{H}\left[\frac{1-x_1}{2}\left\{\frac{5}{2}kT+\frac{h\nu}{\exp(h\nu/kT)-1}\right\}+\frac{3}{2}x_1kT+\frac{x_1}{2}\chi_1\right]$$
$$+\frac{3Y}{8H}kT+avT^4. \tag{A·19}$$

By differenciating Eq. (A·19) we have

$$\left(\frac{\partial\varepsilon}{\partial v}\right)_T=aT^4+\frac{XkT}{2Hv}\frac{x_1(1-x_1)}{2-x_1}\left\{\frac{1}{2}+\frac{\chi_1}{kT}-\frac{h\nu/kT}{\exp(h\nu/kT)-1}\right\}, \tag{A·20}$$

$$\left(\frac{\partial\varepsilon}{\partial T}\right)_v=\frac{kX}{2H}\left[\frac{5+x_1}{2}+(1-x_1)\exp(h\nu/kT)\left\{\frac{h\nu/kT}{\exp(h\nu/kT)-1}\right\}^2\right.$$
$$\left.+\frac{x_1(1-x_1)}{2-x_1}\left\{\frac{1}{2}+\frac{\chi_1}{kT}-\frac{h\nu/kT}{\exp(h\nu/kT)-1}\right\}^2\right]+\frac{3kY}{8H}+4avT^3. \tag{A·21}$$

2) *Ionization of hydrogen atoms and single ionization of helium atoms*

Since these ionization zones overlap each other in the high density region,

the ionization degree x_2 of hydrogen atoms and x_3 of helium atoms are to be calculated from a set of the simultaneous equations

$$\frac{x_2\{Xx_2+(Y/4)x_3\}}{1-x_2}=\frac{H}{h^3}(2\pi m_e kT)^{3/2}v\exp(-\chi_2/kT), \tag{A·22}$$

$$\frac{x_3\{Xx_2+(Y/4)x_3\}}{1-x_3}=\frac{4H}{h^3}(2\pi m_e kT)^{3/2}v\exp(-\chi_3/kT), \tag{A·23}$$

where m_e is the mass of the electron, and $\chi_2(=13.60\text{eV})$ and $\chi_3(=24.58\text{eV})$ are the ionization potentials of the hydrogen atom and the helium atom, respectively. After some calculation, the pressure and the entropy per one atomic mass are expressed as

$$P=\left\{X(1+x_2)+\frac{Y}{4}(1+x_3)\right\}\frac{kT}{Hv}+\frac{1}{3}aT^4, \tag{A·24}$$

$$\begin{aligned}S=&k\left(Xx_2+\frac{Y}{4}x_3\right)\left\{\frac{5}{2}+\ln\frac{2H(2\pi m_e kT)^{3/2}v}{h^3}-\ln\left(Xx_2+\frac{Y}{4}x_3\right)\right\}\\&+k\left(X+\frac{Y}{4}\right)\left\{\frac{5}{2}+\ln\frac{2H(2\pi HkT)^{3/2}v}{h^3}\right\}-kX\,x_2\ln x_2\\&-kX(1-x_2)\ln\frac{1-x_2}{2}-\frac{kYx_3}{4}\ln x_3-\frac{kY}{4}(1-x_3)\ln(1-x_3)\\&+\frac{kY}{4}(2+x_3)\ln 2-kX-\ln X\frac{kY}{4}\ln\frac{Y}{4}+\frac{4}{3}aHvT^3.\end{aligned} \tag{A·25}$$

Further, the internal energy per unit mass is given by

$$\begin{aligned}\varepsilon=&\frac{X}{H}\left\{\frac{3}{2}(1+x_2)kT+\frac{\chi_1}{2}+x_2\chi_2\right\}\\&+\frac{Y}{4H}\left\{\frac{3}{2}(1+x_3)kT+x_3\chi_3\right\}+avT^4.\end{aligned} \tag{A·26}$$

By differenciating Eq. (26) we have

$$\begin{aligned}\left(\frac{\partial\varepsilon}{\partial v}\right)_T=&aT^4+\frac{XkT}{Hv}\frac{x_2(1-x_2)\{Xx_2+(Y/4)x_3\}}{Xx_2(2-x_2)+(Y/4)x_3(2-x_3)}\left(\frac{3}{2}+\frac{\chi_2}{kT}\right)\\&+\frac{YkT}{4Hv}\frac{x_3(1-x_3)\{Xx_2+(Y/4)x_3\}}{Xx_2(2-x_2)+(Y/4)x_3(2-x_3)}\left(\frac{3}{2}+\frac{\chi_3}{kT}\right),\end{aligned} \tag{A·27}$$

$$\begin{aligned}\left(\frac{\partial\varepsilon}{\partial T}\right)_v=&\frac{3kX}{2H}(1+x_2)+\frac{3kY}{8H}(1+x_3)+4avT^3\\&+\frac{kX}{H}x_2(1-x_2)\frac{Xx_2+(Y/4)x_3(2-x_3)}{Xx_2(2-x_2)+(Y/4)x_3(2-x_3)}\left(\frac{3}{2}+\frac{\chi_2}{kT}\right)^2\end{aligned}$$

$$-\frac{kXY}{2H}\frac{x_2(1-x_2)x_3(1-x_3)}{Xx_2(2-x_2)+(Y/4)x_3(2-x_3)}\left(\frac{3}{2}+\frac{\chi_2}{kT}\right)\left(\frac{3}{2}+\frac{\chi_3}{kT}\right)$$

$$+\frac{kY}{4H}x_3(1-x_3)\frac{Xx_2(2-x_2)+(Y/4)x_3}{Xx_2(2-x_2)+(Y/4)x_3(2-x_3)}\left(\frac{3}{2}+\frac{\chi_3}{kT}\right)^2. \qquad (A\cdot 28)$$

3) *Double ionization of heliums*

The ionization degree x_4 of He^+ is determined by

$$\frac{x_4\{X+(Y/4)(1+x_4)\}}{1-x_4}=\frac{H}{h^3}(2\pi m_e kT)^{3/2}ve^{-\chi_4/kT}, \qquad (A\cdot 29)$$

where $\chi_4(=54.40\text{eV})$ is the ionization potential of He^+. The pressure and the entropy per atomic mass are given by

$$P=\left\{2X+\frac{Y}{4}(2+x_4)\right\}\frac{kT}{Hv}+\frac{1}{3}aT^4, \qquad (A\cdot 30)$$

$$S=k\left\{X+\frac{Y}{4}(1+x_4)\right\}\left[\frac{5}{2}+\ln\frac{2H(2\pi m_e kT)^{3/2}v}{h^3}-\ln\left\{X+\frac{Y}{4}(1+x_4)\right\}\right]$$

$$+k\left(X+\frac{Y}{4}\right)\left\{\frac{5}{2}+\ln\frac{2H(2\pi HkT)^{3/2}v}{h^3}\right\}-\frac{kY}{4}x_4\ln x_4$$

$$-\frac{kY}{4}(1-x_4)\ln(1-x_4)+\frac{kY}{4}(3-x_4)\ln 2-kX\ln X$$

$$-\frac{kY}{4}\ln\frac{Y}{4}+\frac{4}{3}aHvT^3. \qquad (A\cdot 31)$$

Finally, the internal energy per unit mass is expressed as

$$\varepsilon=\frac{X}{H}\left(3kT+\frac{\chi_1}{2}+\chi_2\right)+\frac{Y}{4H}\left\{\frac{3}{2}(2+x_4)kT+\chi_3+x_4\chi_4\right\}+avT^4. \qquad (A\cdot 32)$$

By differenciating Eq. (A·32) we have

$$\left(\frac{\partial\varepsilon}{\partial v}\right)_T=aT^4+\frac{YkT}{v}x_4(1-x_4)\frac{X+(Y/4)(1+x_4)}{X+(Y/4)(1+2x_4-x_4^2)}\left(\frac{3}{2}+\frac{\chi_4}{kT}\right), \qquad (A\cdot 33)$$

$$\left(\frac{\partial\varepsilon}{\partial T}\right)_v=\frac{3kX}{H}+\frac{3kY}{8H}(2+x_4)+4avT^3$$

$$+\frac{kY}{4H}x_4(1-x_4)\frac{X+(Y/4)(1+x_4)}{X+(Y/4)(1+2x_4-x_4^2)}\left(\frac{3}{2}+\frac{\chi_4}{kT}\right)^2. \qquad (A\cdot 34)$$

References

1) G. Neugebauer, D. E. Martz and R. B. Leighton, Astrophys. J. **142** (1965), 399.
2) H. L. Johnson, E. E. Mendoza and W. Z. Wisniewski, Astrophys. J. **142** (1965), 1249.
3) F. J. Low and B. J. Smith, Nature **212** (1966), 675.
4) E. E. Becklin and G. Neugebauer, Astrophys. J. **147** (1967), 799.

5) C. Hayashi and T. Nakano, Prog. Theor. Phys. **34** (1965), 754.
6) C. Hayashi, Ann. Rev. Astron. Astrophys. **4** (1966), 171.
7) R. D. Richtmyer, *Difference Methods for Initial-Value Problems* (Interscience Publishers, Inc., New York, 1957).
8) S. A. Colgate and R. H. White, Astrophys. J. **143** (1966), 626.
9) W. D. Arnett, Canad. J. Phys. **44** (1966), 2553.
10) J. E. Gaustad, Astrophys. J. **138** (1963), 1050.
11) S. Chandrasekhar, *An Introduction to the Study of Stellar Structure* (The University of Chicago Press, Chicago, 1939, and Dover Publications, New York, 1957).